INSTITUTE OF PHYSICS PUBLISHING PHYSICS IN MEDICINE AND BIOLOGY

Phys. Med. Biol. **47** (2002) 1721–1731 PII: S0031-9155(02)33433-X

The effect of wall thickness on the response of a spherical ionization chamber

K R Shortt[1], A F Bielajew[2], C K Ross, K J Stewart[3], J T Burke[4] and M J Corsten[5]

Ionizing Radiation Standards, Institute for National Measurement Standards, National Research Council, Ottawa, ON, Canada K1A 0R6

E-mail: carl.ross@nrc.ca

Received 5 February 2002
Published 2 May 2002
Online at stacks.iop.org/PMB/47/1721

Abstract

Air-filled ionization chambers are used widely for radiation dosimetry. For some applications it is important to know the effect on the chamber response of photon attenuation and scattering in the chamber walls. Traditionally, the wall effect is determined by measuring the chamber response as a function of wall thickness and extrapolating linearly to zero thickness. We have constructed a spherical graphite chamber with variable wall thickness. The change in the chamber response with wall thickness has been measured in a ^{137}Cs γ-ray beam. Our data show that the change in response is not linear with wall thickness, in agreement with the theoretical prediction of Bielajew (1990 *Med. Phys.* **17** 583–7). A linear versus non-linear extrapolation of the measured data to zero wall thickness leads to a difference of almost 1% in the estimate of the wall correction factor, K_w. The value of K_w obtained using the non-linear extrapolation is in good agreement with the result obtained using Monte Carlo techniques.

[1] Present address: Dosimetry and Medical Radiation Physics Section, International Atomic Energy Agency, PO Box 100, Wagramer Strasse 5, A-1400 Vienna, Austria.
[2] Present address: Department of Nuclear Engineering and Radiological Sciences, The University of Michigan, Cooley Building, 2355 Bonisteel Boulevard, Ann Arbor, MI 48109-2104, USA.
[3] Present address: Medical Physics Unit, McGill University Health Centre, Montreal General Hospital, 1650 Cedar Avenue, Montreal, QC, Canada H3G 1A4.
[4] Present address: Lawerence Berkeley National Laboratory, 1 Cyclotron Road, Mail Stop 88, Berkeley, CA 94720, USA.
[5] Present address: Newfoundland Cancer Treatment Foundation, Dr H Bliss Murphy Cancer Centre, 300 Prince Philip Drive, St John's NF, Canada A1B 3V6.

0031-9155/02/101721+11$30.00

1. Introduction

Air kerma (or exposure) can be established for photon beams with energies up to about 300 keV using a free-air chamber as a primary standard (Attix 1986). For higher energy beams a free-air chamber becomes impractically large because of the range of the electrons set in motion in air. Thus, cavity chambers with an accurately determined collecting volume are the basis of primary standards for air kerma for photon energies from about 300 keV to about 3 MeV. The chamber wall serves both to define the cavity volume and to establish charged particle equilibrium. However, the wall also scatters and attenuates the incident photon beam, thus perturbing the chamber response from that of an ideal chamber.

Consider a graphite-walled ionization chamber with a gas volume V that is filled with dry air with a mass m_{air}. Let Q_{air} be the charge corresponding to the ions of one sign produced in the air by the ionizing radiation. Then the air kerma is given by (Shortt and Ross 1986)

$$K_{\mathrm{air}} = \frac{(Q_{\mathrm{air}}/e)}{m_{\mathrm{air}}} \frac{W_{\mathrm{air}}}{(1-g)} (\bar{\mu}_{\mathrm{en}}/\rho)_{\mathrm{air,gr}} \bar{s}_{\mathrm{gr,air}} K_{\mathrm{w}} K_{\mathrm{cep}} \prod_i K_i, \tag{1}$$

where W_{air} is the average energy to create an ion pair, e is the electronic charge, g is the fraction of the electron energy lost to radiative processes, $(\bar{\mu}_{\mathrm{en}}/\rho)_{\mathrm{air,gr}}$ is the ratio of the mean mass energy absorption coefficients of air to graphite and $\bar{s}_{\mathrm{gr,air}}$ is the ratio of the mean restricted collisional mass stopping powers of graphite to air. The remaining factors in equation (1) are various corrections to account for the fact that the ionization chamber does not behave like an ideal Bragg–Gray cavity. The two correction factors that are related to wall attenuation and scatter are identified as K_{w} and K_{cep}. There are typically several other small corrections that must be included, such as the effect of stem scatter or the effect of irradiating the chamber in a non-uniform field, but they are not considered in this paper and are grouped together as a product of K_i.

The conventional technique for determining K_{w} is to measure the change in the chamber response as a function of wall thickness and graphically extrapolate the result to zero thickness. Typically, K_{w} amounts to a correction of 1% to 3%, depending on the design of the chamber and its wall thickness. The factor K_{cep} is introduced because the electrons set in motion by the photons have a finite range in the chamber wall[6]. Some of the electrons that contribute to ionization in the cavity gas originate from photon interactions that take place within the wall at a point upstream from the cavity where the photon fluence has not been attenuated by the full wall thickness. Consequently, the extrapolation to zero wall thickness over-corrects for wall attenuation. K_{cep} accounts for this effect and typically amounts to a correction of 0.5% or less. Note that when Monte Carlo techniques are used to determine the wall correction it is the product of K_{w} and K_{cep} that is calculated (Rogers and Bielajew 1990).

In a detailed theoretical study of the wall correction factor for spherical chambers, Bielajew (1990) concluded that the chamber response is not a linear function of the wall thickness. He developed a non-linear theory for the change in response with wall thickness and showed that it was in good agreement with Monte Carlo calculations. Bielajew showed that the non-linearity becomes increasingly severe as the thickness goes to zero. In practice, the wall thickness cannot be reduced below that required to establish charged particle equilibrium. In the case of ^{60}Co γ-rays the non-linearity is expected to be very small over the experimentally accessible range of thicknesses and these data cannot serve as a test of the non-linear theory. The situation for ^{137}Cs is more amenable to experiment because the wall thickness required to establish charged particle equilibrium is only about half of that required for ^{60}Co. Using Monte Carlo calculations, Bielajew and later Corsten (1995) showed that it should

[6] The subscript 'cep' stands for 'centre of electron production'.

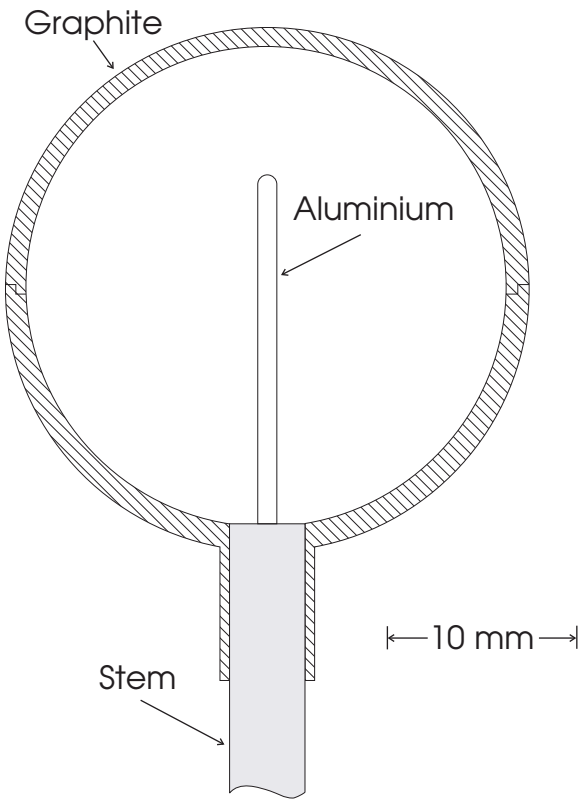

Figure 1. Cross-sectional view of the spherical graphite chamber. It is shown with the thinnest wall. Thicker walls were formed by adding hemispheres from the top and bottom. The hemispheres for the bottom of the chamber were slid down the stem approximately 10 cm when not in use. The top hemispheres were completely removed from the radiation field when not required.

be possible to experimentally test the non-linear theory using a spherical chamber and ^{137}Cs γ-rays.

We have constructed a thin-walled spherical graphite chamber along with a series of spherical shells that can be used to increase the wall thickness. We have measured the change in chamber response as a function of wall thickness using ^{137}Cs γ-rays and compared the results to the non-linear theory. The details of the chamber design and the irradiation protocol are described in section 2. The measured data are compared to the theoretical predictions in section 3.

2. Materials and methods

Figure 1 shows a cross-sectional view of the spherical chamber. It has an inner diameter of 2.54 cm and a volume of 8.6 cm^3. The central electrode is a solid aluminium cylinder, 1 mm in diameter, with a hemispherical end. The chamber wall was constructed from graphite with a density of 1.79 g cm^{-3}. Additional graphite hemispheres were constructed to fit over the chamber. When not used, the top hemisphere of each shell was completely removed from the chamber. The corresponding bottom hemisphere was designed to slide down the stem of the chamber and when not required, it was about 10 cm below the chamber itself.

The ^{137}Cs irradiations were carried out using an Atlan-Tech model GC60 Beam Calibrator system which is described in some detail by Shortt *et al* (1997). The chamber was positioned 1 m from the source where the air kerma rate was approximately 6.7×10^{-2} mGy s^{-1}. The radiation field is circular in cross section, with a diameter of 40 cm at the 1 m position. When the beam is turned on, the source is driven by compressed air from its storage position to the exposed position along a transfer tube. Because the source is not a tight fit in the transfer tube, the source-to-chamber distance may change slightly after each source transit. This variation can lead to an apparent change in the chamber response of a few tenths of 1% and makes it difficult to obtain the precision necessary to observe the expected non-linearity. In order to avoid this problem, a monitor chamber was mounted in the same transverse plane as the spherical chamber but offset from the central axis by about 10 cm. The monitor chamber was a Nuclear Enterprises model 2530 chamber with a collecting volume of 35 cm^3.

Both ionization chamber signals were read using Keithley 35617 electrometers. The air pressure and temperature were monitored so that the chamber response could be corrected for changes in the mass of gas contained within the chamber.

The hemispherical shells in the storage position along the chamber stem can cause scattering that affects the chamber response. In order to measure the effect of shell scattering a jig was set up to permit shells to be mounted above the chamber at the same distance as the shells below the chamber.

3. Results

The chamber current with the beam on was about 20 pA and the leakage current was about 20 fA, or 0.1% of the signal. The leakage was routinely measured and the signal corrected accordingly. The chamber was normally operated with a collecting potential of +300 V. When the polarity was reversed, the signal decreased by 0.09%. When the collecting potential was halved, the signal decreased by 0.29%, leading to a saturation correction of less than 0.1% for 300 V (Weinhous and Meli 1984). These results are typical of what would be expected for a well-designed chamber. The addition of shells to the base chamber decreases the chamber current and leads to a change in the general recombination component of the saturation correction. However, the maximum change in the current was only about 20%, so any change in the saturation correction will be much less than 0.1%. The absolute chamber response was not required for this work and therefore no polarity or saturation corrections were applied to the measured data.

For structural reasons, the central electrode of the chamber was made of aluminium instead of graphite. The effect of the central electrode on chamber response has been studied extensively for the cylindrical NE2571 chamber (Ma and Nahum 1993). In that case, the aluminium electrode increases the chamber response by about 0.6% over the response with a graphite electrode of the same dimensions. Ma and Nahum point out that the main reason for this increase in response is because the aluminium delivers more electrons to the air cavity than a graphite electrode. This suggests that if the size of the chamber is changed, the contribution of the aluminium electrode should scale roughly with the ratio of the surface area of the electrode to the surface area of the chamber wall. Using this approximation, the estimated effect of the aluminium electrode on the spherical chamber response is about 0.1%. Although this estimate applies for ^{60}Co γ-rays, the effect should be similar for ^{137}Cs because the photon and electron interaction coefficients do not change dramatically between the two beam qualities.

Knowledge of the electrode effect would be critical if we were using the spherical chamber as a standard for air kerma. However, it is much less important for the present work where we

Table 1. Measured chamber wall thickness (column 1) and corresponding measured response (column 3). Columns 2 and 4 list the estimated standard uncertainty in the wall thickness and response, respectively. The uncertainties in the wall thickness and the response are combined into an overall uncertainty in the response in column 5. The factor required in the non-linear theory is given in column 6. The response has been arbitrarily normalized to unity for the thinnest wall thickness, and all known corrections have been applied. The graphite used to construct the chamber has a density of 1.79 g cm^{-3}.

Thickness (mm)	Uncertainty (mm)	Response	Uncertainty	Combined uncertainty	$tf(\alpha)$
1.15	0.06	1.0000	0.0010	0.0011	2.47
1.71	0.09	0.9945	0.0005	0.0007	3.38
2.23	0.10	0.9905	0.0009	0.0010	4.16
2.98	0.17	0.9839	0.0011	0.0014	5.25
3.06	0.11	0.9834	0.0004	0.0007	5.36
3.73	0.10	0.9793	0.0008	0.0010	6.26
3.97	0.19	0.9763	0.0011	0.0015	6.57
4.85	0.22	0.9712	0.0011	0.0017	7.71
9.56	0.12	0.9408	0.0008	0.0010	13.31
20.99	0.15	0.8788	0.0003	0.0009	25.70
26.97	0.20	0.8490	0.0018	0.0021	31.94

are studying the change in response with wall thickness. If a large fraction of the ionization in the air cavity were due to the central electrode, we would need to separate the wall and electrode contributions. Because the effect is only about 0.1%, it can be ignored safely.

The wall thickness of the primary graphite shell that defines the chamber volume as well as the thickness of the additional shells was measured at several points over their surfaces. The observed variations in the thickness were used to estimate the standard uncertainty in the total wall thickness as various shells were added. The total wall thickness and its estimated uncertainty for each of the possible chamber configurations are shown in columns 1 and 2 of table 1. The last two chamber configurations with the very thick walls are separated from the rest of the table because they lie outside the range of wall thicknesses most laboratories would use to estimate the wall correction factor.

The effect of scatter on the chamber response from the hemispherical shells stored on the chamber stem varied from zero, when all the shells were mounted on the chamber, to 0.63%, when all the shells were in the storage position. Most of the scatter was due to the two outer shells. The outermost shell is about 6 mm thick and contributed 0.23% to the response, while the next shell is about 11 mm thick and contributed 0.26%. Thus, the effect of scatter on the chamber response was almost constant for the measurements involving the thin shells. The chamber response given in column 3 of table 1 has been corrected for all known effects, including scatter, and arbitrarily normalized to unity for the base chamber. The standard uncertainty in the response was determined from the statistical variation observed over several runs.

Most fitting routines assume that the only significant uncertainty is in the dependent variable. We have used the measured relationship between the response, R, and the wall thickness, t, to estimate a combined uncertainty for R. A simple linear fit to R versus t shows that

$$\Delta R \approx 6.5 \times 10^{-3}\,\Delta t, \tag{2}$$

where Δt is in mm. We then constructed the combined uncertainty in R, σ'_R, as

$$\sigma'_R = \left[\sigma_R^2 + (6.5 \times 10^{-3}\,\sigma_t)^2\right]^{1/2} \tag{3}$$

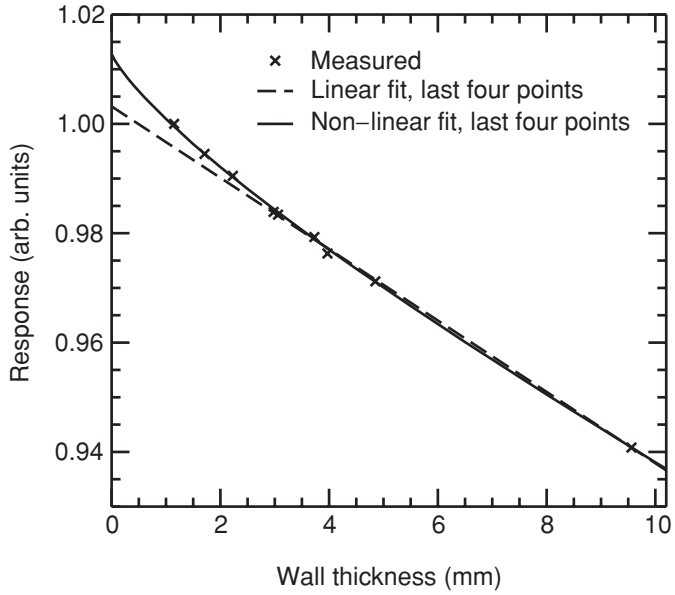

Figure 2. Measured data (crosses), linear fit (dashed line) and non-linear fit (solid line) of the response versus wall thickness for a spherical graphite chamber. The fits were carried out using only the four points lying between 3.5 and 10 on the abscissa. The equations resulting from the fits were used to generate the lines that extend to zero wall thickness.

where σ_R and σ_t are the standard uncertainties in R and t, respectively. This quantity is shown as the fifth column in table 1 and is the uncertainty used in our fitting routine.

Our least-squares fitting routine was taken from Bevington (1969). The routine uses the estimated uncertainties in the values of the dependent variable to construct a weighting factor for each datum point and reports the standard uncertainty in the coefficients obtained from the fit.

The measured response data versus wall thickness are shown in figure 2. The uncertainty bars are not shown in the figure, because they are roughly the same size as the symbols used to represent the data. The dashed line shows the result of a linear fit to the four data points corresponding to wall thicknesses lying between 3.73 mm and 9.56 mm. The rationale for this choice comes from considering the range of thicknesses that have been used to establish air kerma standards. NIST (formerly NBS) used wall thicknesses from about 3.6 mm to 6.7 mm to establish the wall correction factors for its spherical chambers for both ^{60}Co and ^{137}Cs γ-rays (Loftus and Weaver 1974). NRC used thicknesses from about 3 mm to 7 mm to determine the correction factor for the cylindrical chamber that is the basis of its ^{60}Co standard (Shortt and Ross 1986). The coefficients from the fit as well as the value of K_{w} for a chamber with a wall thickness of 3.6 mm are shown in table 2.

The measured data in figure 2 show the same trend for small values of the wall thickness as predicted by Bielajew (1990) using Monte Carlo calculations. That is, the response increases more rapidly than predicted by the linear fit as the thickness goes to zero. Bielajew went on to develop an analytic theory to explain the non-linearity and it predicts that the chamber response should vary with wall thickness according to

$$R(t) = a_0 + a_1 t f(\alpha), \tag{4}$$

Table 2. Results from the different methods of determining the wall correction factor. The coefficients a_0 and a_1 were determined for both the linear and non-linear theories by fitting the four data points corresponding to wall thicknesses between 3.73 mm and 9.56 mm. K_w was evaluated for a chamber with a wall thickness of 3.6 mm. The Monte Carlo result is taken from Corsten (1995). The results in the last two rows include the data for the very thick chamber walls. The χ^2/ν statistic was computed using all the data points shown in figure 3 (rows 2 and 3) or figure 4 (rows 5 and 6). The standard uncertainty is given in parentheses.

	a_0	a_1	χ^2/ν	K_w
Linear (figures 2 and 3)	1.0032 (0.0015)	-6.53×10^{-3} (0.22×10^{-3})	4.4	1.0240 (0.0023)
Non-linear (figures 2 and 3)	1.0128 (0.0018)	-5.41×10^{-3} (0.18×10^{-3})	0.17	1.0336 (0.0021)
Monte Carlo	–	–	–	1.0313 (0.0008)
Linear (figure 4)	0.9984 (0.0008)	-5.69×10^{-3} (0.06×10^{-3})	20.3	1.0210 (0.0011)
Non-linear (figure 4)	1.0102 (0.0010)	-5.11×10^{-3} (0.05×10^{-3})	1.9	1.0318 (0.0014)

where a_0 and a_1 are constants. The slope correction function, $f(\alpha)$, is given by

$$f(\alpha) = [1 + (1 + 1/(2\alpha)) \ln(1 + 2\alpha)]/2, \tag{5}$$

where α is equal to r/t, and r is the chamber radius. Although $f(\alpha)$ diverges as t goes to zero, the product $tf(\alpha)$ appearing in equation (4) goes to zero. The values of $tf(\alpha)$ for our chamber are given in column 6 of table 1.

The coefficients a_0 and a_1 were obtained by fitting equation (4) to the same four data points used for the linear fit. The resulting equation for $R(t)$ is plotted as the solid line in figure 2, and the coefficients are given in table 2. Figure 2 indicates that the non-linear theory fits the measured data quite well. In order to better assess the quality of the fit, the data in figure 2 have been re-plotted in figure 3 by dividing the value of the response for each wall thickness (either measured or fitted) by the value obtained from the linear fit. The expanded scale in figure 3 permits the uncertainty bars to be displayed and the figure clearly shows how the measured response deviates from the linear theory for small wall thicknesses. It also shows that the non-linear theory fits the measured data within the estimated uncertainties. For a chamber with a wall thickness of 3.6 mm, the non-linear theory predicts a value for K_w that differs by 0.94% from that obtained using a linear fit.

Table 1 also reports results that we obtained for two wall thicknesses much greater than would normally be used for determining K_w. Both the linear and non-linear fits were re-done, this time including the two additional points. The coefficients from the fits are given in table 2 and the results are displayed in figure 4. By comparing figures 3 and 4, one can see that the linear theory breaks down, not only for thin walls, but for thick walls as well. The non-linear theory does considerably better at fitting the measured data although the fit is not as good as in figure 3. Corsten (1995) carried out Monte Carlo studies for spherical chambers with wall thicknesses of more than 80 mm. Her calculations showed that the non-linear theory begins to break down as the wall thickness becomes very large. This is qualitatively the same effect as shown in figure 4.

The reason the theory begins to fail for large wall thicknesses is that one of its underlying assumptions is no longer fulfilled. To simplify the mathematics, Bielajew assumed that a first-order expansion of the exponential photon attenuation factor would be adequate. This requires that $\mu_{\text{eff}} t \ll 1$, where μ_{eff} is the effective photon attenuation coefficient. According to equation (2) in Bielajew (1990), $\mu_{\text{eff}} = -a_1/a_0$, where a_0 and a_1 are the coefficients for the non-linear fit given in table 2. If we require that $\mu_{\text{eff}} t$ be less than 0.1, then t must be less than 19 mm. This estimate is in reasonable agreement with the results presented in figure 4, which suggest that the theory begins to fail at a wall thickness of about 15 mm.

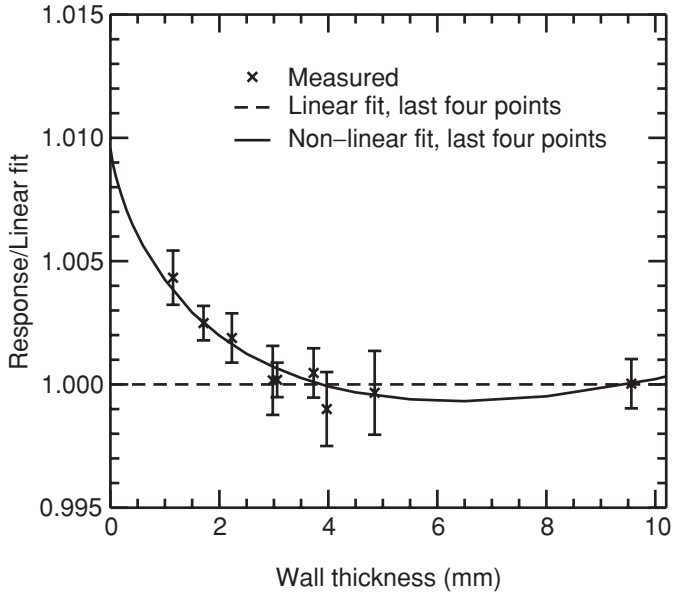

Figure 3. Same as figure 2, except that the results for each wall thickness have been divided by the value of the linear fit for that thickness.

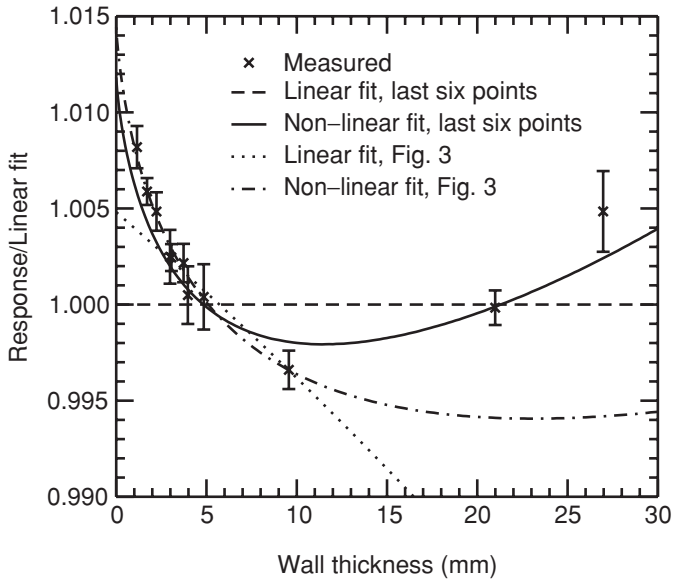

Figure 4. Same as figure 3, except that the additional data for the thick walls have been included in the fits. The four-point fits from figure 3 are also shown. The results for each wall thickness have been divided by the value of the six-point linear fit for that thickness.

The four-point fits from figure 3 are also shown in figure 4, except that now they are referenced to the six-point linear fit. The datum point for the thickest wall deviates by more than 2% from the four-point linear fit. The four-point non-linear fit reduces this discrepancy

by about a factor of 2. The quality of the various fits can be assessed more quantitatively using the reduced chi-square statistic (χ^2/ν) given in table 2. The value of χ^2/ν for the four-point non-linear fit is more than a factor of 10 smaller than the value for the next best fit, which is the six-point non-linear case. Even though the quality of the six-point non-linear fit deteriorates significantly when the thick-wall data points are included, the value of K_w changes only by about 0.2%.

Table 2 reports a value of K_w obtained from a Monte Carlo calculation. As mentioned in the introduction, the Monte Carlo technique calculates the quantity $K_w K_{cep}$, and thus a value of K_{cep} is needed to permit a comparison of measured and calculated values of K_w. According to Loftus and Weaver (1974), K_{cep} for ^{137}Cs is 0.999, and this value has been used to extract K_w from the Monte Carlo calculation. The value of K_w reported in table 2 has been taken from Corsten (1995) and was obtained using the EGS4 Monte Carlo code (Nelson *et al* 1985).

4. Conclusions

The effect of wall attenuation and scatter is one of the most important corrections that must be determined when using a cavity chamber as an air kerma standard. Usually the correction has been estimated by linearly extrapolating the measured response versus wall thickness to zero thickness. Bielajew (1990) developed an analytic theory that showed that the extrapolation is non-linear and used Monte Carlo calculations to support the model. In order to experimentally test his work, we constructed a spherical chamber with a thin wall, as well as a series of shells that could be used to systematically change the wall thickness. Figures 2 and 3 clearly show that the non-linear theory is a much better fit to the measured data than the linear theory. The figures also demonstrate that, in the range of wall thicknesses (3 to 10 mm) normally used for extrapolation, there is no significant difference between the linear and non-linear theories.

Wall thicknesses of more than 10 mm have normally not been used in fitting the measured response versus wall thickness. We have included data for wall thicknesses of more than 25 mm to demonstrate that, if thicker walls had been used, non-linearities would have become apparent (figure 4). Although the thick-wall data do not provide much guidance on how to extrapolate to zero wall thickness, they would have called into question the validity of a linear extrapolation.

Figure 3 indicates that if only the data for wall thicknesses less than about 3 mm were used in a linear fit, the value obtained for K_w would be close to the true value. However, Loftus and Weaver (1974) used the same range of wall thicknesses (i.e. 3.6 mm to 6.7 mm) for both ^{137}Cs and ^{60}Co γ-rays in their work with spherical ionization chambers and thus were not aware of the curvature that becomes apparent as the wall thickness is decreased. For ^{60}Co, the region where the curvature becomes large is not experimentally accessible because the minimum wall thickness to establish full build-up is about 3 mm. In this case, there is no option for using a straight line to accurately determine the response versus wall thickness as the thickness goes to zero.

Bielajew's analytic form of the slope correction function (equation (5)) only applies to spherical chambers. However, the model used to derive this function can be applied to other chamber geometries, although the relevant integrals may need to be evaluated numerically. The French standards laboratory (Laboratoire National Henri Becquerel, or LNHB) has taken this approach to evaluate K_w for its air kerma standard which is based on a cylindrical graphite chamber with hemispherical end caps (Delaunay *et al* 1993). Shortt *et al* (2001) have compared the air kerma standards of the LNHB and the National Research Council of Canada (NRC) and found that the ratio of the LNHB standard to that of NRC is 1.001 ± 0.004. The wall correction factor for the cylindrical graphite chamber that is the basis of the NRC standard was obtained from a Monte Carlo calculation, so this result is an indirect indication that the

Bielajew model and the Monte Carlo technique give consistent values for the wall correction factor.

Our results provide a direct comparison between the non-linear theory and the Monte Carlo method for the same chamber. The results in table 2 show that, for our spherical graphite chamber, the value of K_w obtained by non-linear extrapolation is in very good agreement with that obtained by the Monte Carlo calculation. This result adds support to the perspective (Bielajew 1990) that the Monte Carlo technique is the best approach for determining the wall correction factor for an arbitrary chamber.

Our measurements have been carried out using ^{137}Cs γ-rays, even though air kerma standards for ^{60}Co are much more important because of their use in dosimetry protocols. The question then arises as to whether or not conclusions regarding wall extrapolation data for ^{137}Cs are also relevant for ^{60}Co. As pointed out in the introduction, we could not use ^{60}Co γ-rays because the requirement for charged particle equilibrium means that the non-linear region is not experimentally accessible. However, Bielajew (1990) has used Monte Carlo calculations and his non-linear theory to compare the response of a spherical chamber to ^{60}Co and ^{137}Cs γ-rays. Figures 4 and 5 in his paper show that the chamber response versus wall thickness is similar for both beam qualities. Thus, we conclude that the non-linear behaviour observed with ^{137}Cs γ-rays is compelling evidence that the response versus wall thickness is non-linear for ^{60}Co as well.

Rogers and Bielajew (1990) and Bielajew and Rogers (1992) have used Monte Carlo calculations to re-evaluate the wall correction factors for most of the primary standards for air kerma. The Monte Carlo calculations lead to changes in the wall correction factor of up to 1%. The German standards laboratory has recently announced that it is changing its ^{60}Co and ^{137}Cs air kerma standards by almost 1% as a result of a Monte Carlo re-evaluation of its wall correction factors (Kramer *et al* 2001). Our results support the perspective that it is difficult to determine K_w with high accuracy using only measurements of the change in chamber response with wall thickness.

Acknowledgments

David Marchington was instrumental in the design and construction of the spherical ionization chamber. He also played a major role in establishing and maintaining the ^{137}Cs irradiation facility. Dr F Delaunay of LNHB provided many useful comments on various aspects of this work.

References

Attix F H 1986 *Introduction to Radiological Physics and Radiation Dosimetry* (New York: Wiley)

Bevington P R 1969 *Data Reduction and Error Analysis for the Physical Sciences* (New York: McGraw-Hill) pp 171–6

Bielajew A F 1990 On the technique of extrapolation to obtain wall correction factors for ion chambers irradiated by photon beams *Med. Phys.* **17** 583–7

Bielajew A F and Rogers D W O 1992 Implications of new correction factors on primary air kerma standards in ^{60}Co-beams *Phys. Med. Biol.* **37** 1283–91

Corsten M J 1995 Ionization chamber response for brachytherapy sources *MSc Thesis* Carleton University, Ottawa

Delaunay F, Chauvenet B and Simoën J P 1993 Caractérisation primaire en débit de kerma dans l'air du faisceau de ^{60}Co n II B (Détermination de différents facteurs) *Note Technique* LPRI/93/013 (Saclay: Laboratoire National Henri Becquerel)

Kramer H M, Büermann L and Ambrosi P 2001 The magnitude of the unit of Gray *Radiat. Prot. Dosim.* **97** 287–8

Loftus T P and Weaver J T 1974 Standardization of ^{60}Co and ^{137}Cs gamma-ray beams in terms of exposure *J. Res. Natl. Bur. Stand.* A **78** 465–76

Ma C M and Nahum A E 1993 Effect of size and composition of the central electrode on the response of cylindrical ionization chambers in high-energy photon and electron beams *Phys. Med. Biol.* **38** 267–90

Nelson W R, Hirayama H and Rogers D W O 1985 *The EGS4 Code System* SLAC-265 (Stanford, CA: Stanford Linear Accelerator Laboratory)

Rogers D W O and Bielajew A F 1990 Wall attenuation and scatter corrections for ion chambers: measurements versus calculations *Phys. Med. Biol.* **35** 1065–77

Shortt K R and Ross C K 1986 The Canadian ^{60}Co exposure standard *NRC Report* PIRS-0052 (Ottawa: National Research Council)

Shortt K R, Ross C K and Janovský I 1997 The response of LiF TLDs to ^{137}Cs and ^{60}Co γ rays *Radiat. Prot. Dosim.* **69** 257–66

Shortt K, Ross C, Seuntjens J, Delaunay F, Ostrowsky A, Gross P and Leroy E 2001 Comparison of dosimetric standards of Canada and France for photons at ^{60}Co and higher energies *Phys. Med. Biol.* **46** 2119–42

Weinhous M S and Meli J A 1984 Determining P_{ion}, the correction factor for recombination losses in an ionization chamber *Med. Phys.* **11** 846–9